http://dx.doi.org/10.5012/bkcs.2013.34.3.979

Dithienosilole Based Organic Sensitizers for Efficient Dye-Sensitized Solar Cells

Jungeun Park, Eunji Lee, Jinho Kim, and Youngjin Kang*

Division of Science Education & Department of Chemistry, Kangwon National University, Chuncheon 200-701, Korea
**E-mail: kangy@kangwon.ac.kr*
Received December 10, 2012, Accepted December 20, 2012

Key Words : Dithienosilole, Dye-Sensitized Solar Cells (DSSCs), Bulky spacer, Photon to current conversion efficiency

Recently, organic sensitizers-based dye sensitized solar cells (DSSCs) have attracted much attention due to their several advantages such as low cost preparation, structural diversity, and high power conversion efficiency (η: 8-9%).[1] Organic sensitizers consist typically of three segments of donor, π-linker, and acceptor (D-π-A), which are shown to have efficient intramolecular charge transfer (ICT) characteristics.[2] Particularly, organic sensitizers bearing dithienosilole (DTS) as a π-linker have shown to have high efficiencies (η: 7.6-10.5%) in DSSCs performance due to its unique photophysical properties (σ^*-π^* conjugation)[3] and coplanarity.[2,4,5] In addition, the efficiency in DSSC performance is a quite sensitive depending on the nature of substituents at 3-position of DTS ring. For examples, the bulky substitution on silicon atom of DTS ring may reduce the π-π stacking interactions of dyes and may be beneficial to high electron injection yield and the power conversion efficiency.[2,5] These facts prompted us to develop new organic dyes containing DTS π-linker and investigate the effect of bulky substituent at 3-position of DTS ring in DSSC performance. Herein, we report the results of our investigation on the preparation, photophysical properties, electrochemical behavior, and DSSC performance of two novel DTS dyes.

Result and Discussion

Two DTS based dyes **1** and **2** were obtained in moderate yields *via* three step processes that involved first the Negishi[6] coupling of *N*-(4-bromophenyl)-*N,N*-bis(9-phenyl-9*H*-carbazol-3-yl)amine with corresponding bromotrime-thylsilyl-dithienosiloles **A-B**, followed by formylation and Knoevenagel condensation with cyanoacetic acid in the presence of a catalytic amount of piperidine in acetonitrile and chloroform, as shown in Scheme 1. The molecular structures of **1** and **2** were confirmed using varied spectroscopic methods, such as NMR, mass and elemental analysis. All compounds are black dyes and fairly stable under air and moisture both in solution and in the solid state. Figure 1 exhibits the absorption and emission spectra of **1** and **2** sensitizers measured in THF at ambient temperature.

All compounds show two intense absorption bands and their maximum values (λ_{max}) are observed at *ca.* 200-300 and 400-550 nm, respectively, as shown in Table 1. This absorption pattern is similar to those of DTS based organic

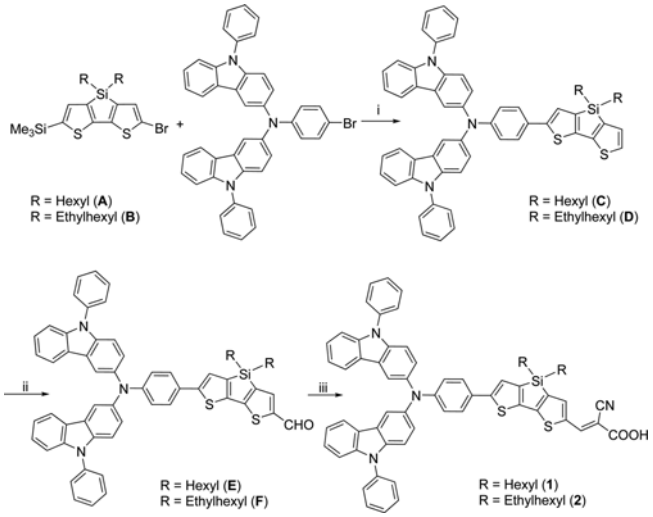

Scheme 1. Reagent and conditions: i) *n*-BuLi, $ZnCl_2$(tmeda), $Pd(PPh_3)_4$, reflux, 12 h, THF. ii) $POCl_3$, DMF, 0 °C, 10 min; 80 °C, 5 h. iii) cyanoacetic acid, piperidine, $CH_3CN/CHCl_3$, 80 °C, 10 h.

dyes, such as 3-{5-[4-(*N,N*,-bis(9,9-dimethylfluoren-2-yl))-phenyl]-3,3'-dimethyl silylene-2,2'-bithiophene-5'-yl}-2-cyano-acrylic acid (**DTS-Me$_2$**) and 3-{5-[4-(*N,N*,-bis(9,9-dimethyl fluoren-2-yl)phenyl]-3,3'-diphenylsilylene-2,2'-bithiophene-5-yl}-2'-cyano acrylic acid (**DTS-Ph$_2$**), which look very much like **1**-**2** in structural aspect except donor and bulky π-

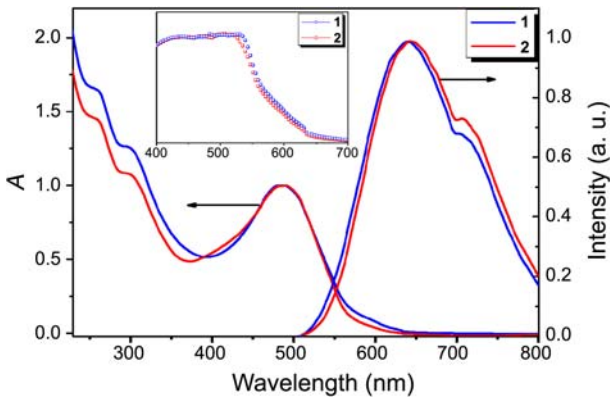

Figure 1. Absorption and emission spectra of **1** (blue) and **2** (red) in THF at ambient temperature. Inset: Absorption spectra of 1 and 2 absorbed on TiO_2 film.

Table 1. Optical, redox, and DSSC performance parameters of **1** and **2**

Dye	λ_{abs}[a] [nm] (ε [$M^{-1}cm^{-1}$], $\times 10^4$)	E_{ox}[b] [V]	$E_{0\text{-}0}$[c] [V]	E_{LUMO}[d] [V]	J_{sc} [$mAcm^{-2}$]	V_{oc} [V]	*ff*	η[e] [%]
1	206 (10), 299 (8.0), 486 (6.4)	1.25	2.23	-0.77	15.2	0.62	0.70	6.71
2	259 (5.4), 300 (4.0), 490 (3.7)	1.17	2.22	-1.06	14.4	0.74	0.70	6.58
N719					14.2	0.78	0.75	8.38

[a]The absorption spectra were measured in THF solution. [b]The redox potentials of the dyes on TiO_2 were measured in CH_3CN with 0.1 M $(N\text{-}C_4H_9)_4NPF_6$ at a scan rate of 50 mVs^{-1} (*vs*. NHE). [c]$E_{0\text{-}0}$ was determined from the intersection of the absorption and emission spectra in THF. [d]E_{LUMO} was calculated by E_{ox}-$E_{0\text{-}0}$. [e]The performances of the DSSCs were measured using a working area of 0.18 cm^2. Electrolyte: 0.6 M DMPImI, 0.05 M I_2, 0.1 M LiI, and 0.5 M *tert*-butylpyridine in CH_3CN.

linker.[7] For **1** and **2**, the first band at shorter wavelength shows much stronger absorption than the second band at longer wavelength. However, there is a big difference in molar extinction coefficient. The difference of molar extinction coefficient between two intense bands (λ = 367 nm and λ = 504 nm) in **DTS-Me$_2$** is *ca*. 19,000 dm^3 mol^{-1} cm^{-1}, while larger differences of molar extinction coefficient in **1** (17,000 dm^3 mol^{-1} cm^{-1}) and **2** (36,000 dm^3 mol^{-1} cm^{-1}). This observation can be due to the introduction of bulky π-linker. In general, an intense absorption band of silole derivatives, which is attributed to the π-π^* transition of central five-memberd silole ring, appears at 300-400 nm.[8]

Therefore, it can be assigned that two intense absorption band is attributed to the π-π^* transition of carbazole-functionalized amine groups involving π-π^* transition of dithienosilole linker. Under the same molar concentration, compound **1** that contains dihexyl moiety at 3-position of dithienosilole ring exhibits stronger and blue-shifted absorption band at 486 nm (ε = 64000 dm^3 mol^{-1} cm^{-1}) as compared to compound **2**, indicating that less bulky hexyl substituents than ethylhexyl brings about effective π-conjugation throughout molecular structure. The absorption bands of **1** and **2** onto a TiO_2 electrode are relatively broadened and tail off at about 650 nm, which can account for the black color of DTSs (Inset in Fig. 1). Such broadening and red-shifted absorption have been reported in other organic dyes on TiO_2 electrodes.[7] Upon irradiation of UV light (354 nm), compounds **1** and **2** display strong red emission in solution at ambient temperature. Interestingly, compound **2** emits at λ_{max} = 643 nm, about 10 nm red-shifted, compared to that of **1** (λ_{max} = 635 nm), which can be explained by the structural difference at 3,3-position of DTS ring and bulkiness of substituents between these two molecules. When **1** and **2** are adsorbed onto a nanocrystalline TiO_2 film, the emission bands were not observed in the region of 500-800 nm. This observation suggests that the electron injection from an excited state of dye to TiO_2 occurs efficiently.

To gain deeper insight into the geometrical configuration and the nature of luminescence exhibited by **1** and **2**, we carried out molecular orbital calculations $S_0 \rightarrow S_1$ excitation energy calculations for the two compounds in the gas phase using Gaussian 03 package.[9] Figure 2 shows optimized structure and the HOMO and LUMO levels of **1** and **2**. The torsional angles between the phenyl ring attached to the nitrogen atom and the DTS plane in the optimized structures of **1** and **2** are 19.8°, and 20.9°, respectively. Due to the ethylhexyl groups attached to the 3-position of the DTS ring, the torsional angles in **2** are slightly larger than in **1**. This fact indicates that the phenyl ring attached on nitrogen atom is almost coplanar with DTS ring, leading to effective π-conjugation throughout molecules. Figure 3 presents the isodensity plots of the frontier molecular orbitals of **1** and **2**. The HOMO levels of the dye molecules are mainly dominated by π orbital contribution of 9-phenylcarbazole unit with a small contribution from the DTS ring p orbital. However, the LUMO levels are nearly a π^* orbital with dominating contributions from the DTS ring and the cyanoacrylic groups and the LUMO+1 levels is also a π^* orbital mainly delocalized across the DTS ring and the cyanoacrylic groups.

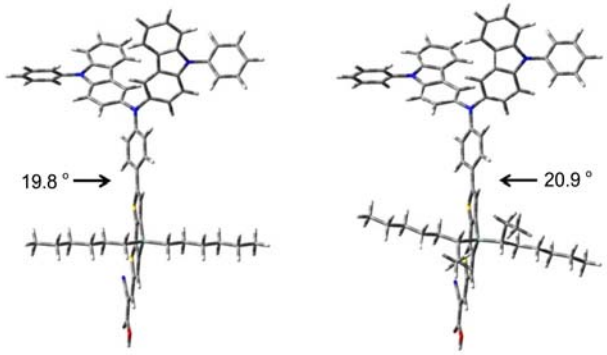

Figure 2. Optimized molecular structure of **1** (left) and **2** (right) at the B3LYP/6-31G(d) level.

The HOMO, and LUMO of **1** and **2** have the shapes similar to those of **DTS-Me$_2$** and **DTs-Ph$_2$**.[7] This result implies that DTS ring has a great deal of influence on even LUMO+1 level as well as LUMO level.

Table 2 shows the calculated $S_0 \rightarrow S_1$ vertical excitation energies along with the oscillator strength and the transition orbitals having the maximum CI coefficients for dyes **1** and **2**. The calculated excitation energies are also compared with the experimental absorption maxima. It is found out that the calculated excitation energies are more red-shifted than the measured absorption bands of the compounds. This may be caused by the fact that the measurements were conducted in THF while the calculations were carried out *in vacuo*.

The transition orbitals and considerable magnitude of oscillator strengths as well as the isodensity surface plots of the HOMO and LUMO indicate that the measured absorption and emission of compounds **1** and **2** are originated from $\pi \rightarrow \pi^*$ transitions between the 9-phenylcarbazole and the

Table 2. Calculated $S_0 \rightarrow S_1$ excitation energies (E), oscillator strength (f), configuration compositions with CI coefficient larger than 0.1, and experimental absorption band maxima

Molecule	E (eV/nm)	f	Composition (CI coefficient)	Exp. (nm).
1	1.98 / 627	0.787	HOMO → LUMO (0.89)	486
2	1.98 / 626	0.764	HOMO → LUMO (0.89)	490

cyanoacrylic group with a contribution of the DTS ring. Based on experimental and theoretical results, we believe that the absorption and emission of compounds **1** and **2** are originated from 9-phenylcarbazole and cyanoacrylic groups-based π-π^* transition with the contribution of DTS ring. In addition, this result for the change of electron distribution in HOMO and LUMO level supports an efficient charge separation of DTS dyes.

The both **1** and **2** adsorbed on TiO_2 films show a single reversible oxidation at 1.25 V and 1.17 V (*vs* NHE), respectively. In addition, the separation potentials between anodic peak (E_{pa}) and cathodic peak (E_{pc}) for **1** and **2** are 0.50 V and 0.27 V, respectively (See ESI). This reversible process can be assigned to the oxidation of 9-phenylcarbazole, as supported by our previous report.[3b,7] The reduction potentials of three dyes calculated from the oxidation potentials and the $E_{0\text{-}0}$ determined from the intersection of absorption and emission spectra are listed in Table 1. The LUMO energies of **1** and **2** are −0.77 and −1.06 (*vs* NHE), respectively. These energies are similar or higher than those of **DTS-Me$_2$** (−1.05 V) and **DTSPh$_2$** (−1.20 V). This lowering of LUMO energies permits the electron in the excited state of dye to be effective injected the conduction band of TiO_2 (−0.5 V *vs* NHE).

Figure 4 shows the action spectra of monochromatic incident photon-to-current conversion efficiencies(IPCEs) for DSSCs based on **1** and **2**. The onset wavelengths of IPCE spectra for DSSCs based on **1** and **2** are 750 and 740 nm, respectively. The **1** sensitizer IPCE spectrum is red-shifted by about 10-20 nm as compared to **2**. The observed IPCE

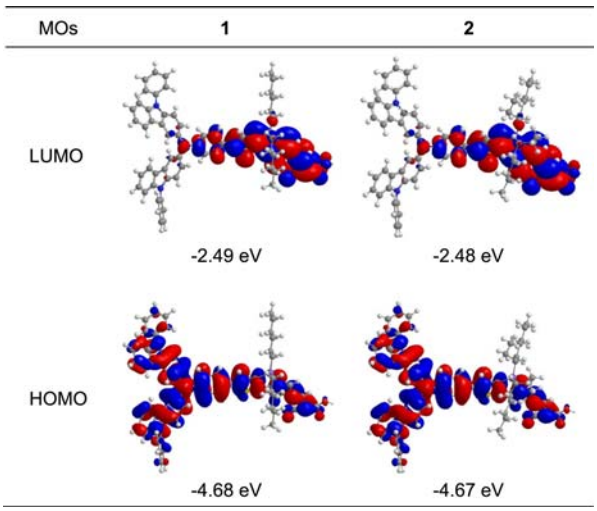

Figure 3. Isodensity surface plots and energies of the HOMO and LUMO of **1** and **2** (isodensity contour = 0.03 a. u.).

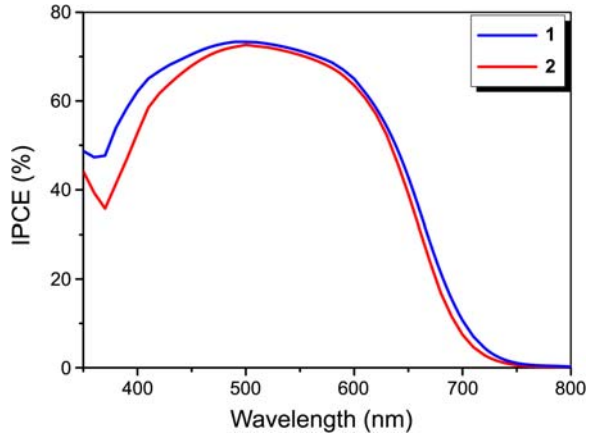

Figure 4. Action spectra of incident photon-to-current conversion efficiency (IPCE) for DSSCs based on **1** and **2**.

value for the DSSCs based on **1** and **2** is more than 70% in the region of 450-560 nm (maximum value, **1**: 74% at 490; **2**: 73% at 500 nm), indicating the efficient DSSCs performance.

Under standard global AM (Air Mass) 1.5 solar condition, the **1** sensitized cell gave a short circuit photocurrent density (J_{sc}) of 15.2 mA/cm^2, an open circuit voltage(V_{oc}) of 0.62 V, and a fill factor of 0.70, corresponding to an overall conversion efficiency η, derived from the equation J_{sc}·V_{oc}:*ff*/light intensity, of 6.71% (See Figure 5). By contrast, the conversion efficiency of **2** based DSSCs are 6.58%, which is lower than those of **1** and **N-719**[10] (*cis*-di(thiocyanato)-*N*,*N*′-bis(2,2'-bipyridyl-4-carboxylic acid-4'-tetrabutyl ammonium carboxylate) ruthenium(II)) sensitized cell under the same condition (J_{sc}: 14.4 mA/cm^2, V_{oc}: 0.74 V, *ff*: 0.70 for **2**; J_{sc}: 14.2 mA/cm^2, V_{oc}: 0.78 V, *ff*: 0.75 for **N-719**). The better J_{sc} of DTS dyes than that of N-719 implies that the electron injection to the conduction band of TiO_2 occurs easily due to the diminution of LUMO energy. It is noteworthy that the V_{oc} for DSSC based on **2** sensitizer, which contains bulky ethylhexyl groups at 3-position of DTS ring, is higher than that for **1**.

The effects of the bulky hexyl or ethylhexyl chains on photovoltaic characteristics were further elucidated by

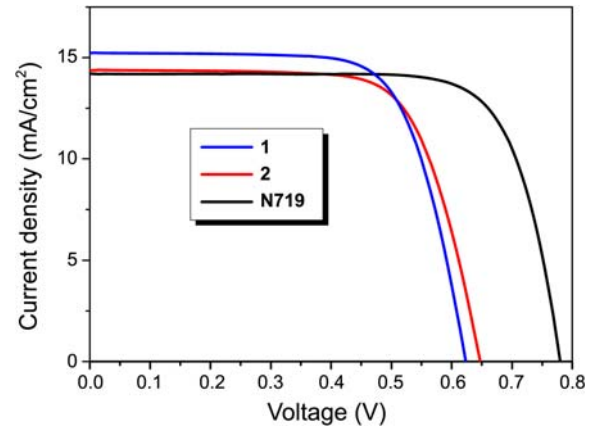

Figure 5. A photocurrent voltage curve obtained with a DSSC based on **1** (blue line), **2** (red line) and **N-719** (black line) under AM 1.5 radiation.

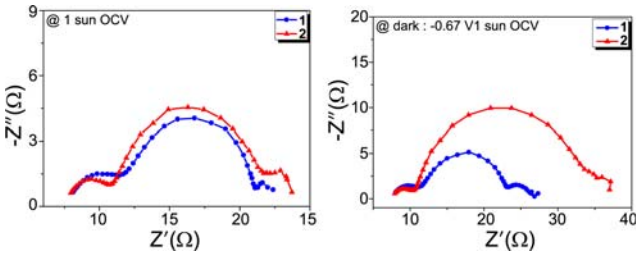

Figure 6. Electrochemical impedance spectra measured the illumination (1 sun, top) and the dark (bottom) for cell with **1** (blue circle) and **2** (red triangle) dye adsorption conditions.

electrochemical impedance spectroscopy (EIS). Figure 6 shows the EIS Nyquist plots (*i.e.*, minus imaginary part of the impedance -*Z* *vs* the real part of the impedance *Z* when sweeping the frequency) for DSSCs based on **1** and **2** dyes.

Figure 6 shows the impedance spectra measured under illumination and dark conditions. Upon illumination of 100 mW/cm^2 under open circuit condition, the radius of intermediate frequency semicircle in the Nyquist plot decreased in the order of **2** (10.43 Ω) > **1** (8.88 Ω), indicating fact that compound **1** shows the improvement of charge generation and transport. As the comparison of short circuit photocurrent between **1** and **2**, this result is consistent with fact that compound **1** has higher J_{sc} value than in compound **2**, as shown in Table 1. In the dark under forward bias (−0.67 V), the radius of the intermediate frequency semicircle showed the increasing order of **2** (22.65 Ω) > **2** (11.03 Ω), in accordance with the trends of the V_{oc} in **1** and **2**.

In summary, we designed and synthesized two DTS based organic dyes (**1** and **2**) with bulky alkyl groups. To investigate their photon-to-current efficiencies, DSSCs using two dyes were fabricated. All compounds showed more than 6% efficiencies, in which their performances are sensitive depending on the structure of dyes. Particularly, the efficiency of compound **1** with bulky hexyldithienosilole as a π-linker was marked over 80% of that of N-719.

Experimental

Materials and Characterization. The several of dithienosilole spacers and key starting material were prepared as described in literature.[2] The synthetic details of intermediates (**A**-**F**) are described in supporting information.

General Synthesis of 1 and 2. A mixture of corresponding aldehyde (0.73 mmol) and cyanoacetic acid (1.46 mmol) was vacuum dried and MeCN/$CHCl_3$ (60 mL/30 mL) and piperidine (0.22 mmol) were added. The mixture was refluxed for 10 h. After cooling the reaction mixture, all volatiles were removed in vacuo. The pure products were obtained by column chromatography (silica) in 57-58% yield.

Compound 1: Eluent:Hexane/THF/EtOH (1:1:1, v/v); Yield: 57%, black solid. ^{1}H-NMR (DMSO-d_6, 300 MHz) δ 8.15 (t, J = 8.0 Hz, 4H), 8.12-7.30 (m, 24H), 6.90 (t, J = 8.8 Hz, 2H), 1.37-0.90 (m, 22H), 0.88 (t, J = 7.6 Hz, 4H). ^{13}C-NMR (DMSO-d_6, 100 Hz) 206.8, 141.0, 139.5, 137.7, 137.1, 130.5, 128.0, 127.0, 126.8, 125.7, 124.1, 122.8, 120.4, 40.3, 40.3, 40.1, 39.7, 39.5, 39.3, 34.7, 32.3, 31.1, 31.1, 30.8, 23.1, 22.3, 21.4, 14.2, 11.4. Mass (*m/z*): 1030.41. Anal. Calcd for $C_{66}H_{58}N_4O_2S_2Si$: C, 76.86; H, 5.67; N, 5.43; found: C 76.90, H 5.59, N 5.42.

Compound 2: Eluent:Hexane/THF/EtOH (1:1:1, v/v); Yield: 58%, black solid. ^{1}H-NMR (DMSO-d_6, 300 MHz) δ 8.17 (m, 2H), 7.75-7.35 (m, 10H), 6.87 (s, 3H), 6.67 (s, 1H), 1.35 (s, 26H), 0.69 (s, 9H). ^{13}C-NMR (DMSO-d_6, 100 Hz) 161.7, 140.6, 136.8, 131.6, 131.2, 129.1, 127.8, 127.7, 127.5, 126.7, 126.1, 125.3, 123.5, 122.3, 119.6 129.1, 120.9, 109.1, 35.5, 34.8, 33.8, 33.7, 31.2, 30.3, 29.3, 28.9, 28.6, 28.1, 27.9, 26.3, 22.4, 22.2, 21.9, 20.8, 20.1, 13.2, 13.1, 9.7. Mass (*m/z*): 1086.44. Anal. Calcd for $C_{70}H_{66}N_4O_2S_2Si$: C, 77.31; H, 6.12; N, 5.15; found: C 77.28, H 6.11, N 5.19.

Acknowledgments. This research was supported by Basic Science Research Program through the National Research Foundation of Korea (NRF) funded by the Ministry of Education, Science and Technology (2011-0010518) and the industrial strategic technology development program (10039141) funded by the Ministry of Knowledge Economy (MKE, Korea).

Supporting Information. Synthetic details of starting materials, NMR, and mass spectra.

References

1. Recent review: (a) Gong, J.; Liang, J.; Sumathy, K. *Renew. Sust. Energ. Rev.* **2012**, *16*, 5848. (b) Hagfeldt, A.; Boschloo, G.; Sun, L.; Kloo, L.; Pettersson, H. *Chem. Rev.* **2010**, *110*, 6595. (c) Mishra, A.; Fischer, M. K. R.; Bäuerle, P. *Angew. Chem., Int. Ed.* **2009**, *48*, 2474.
2. Lin, L.-Y.; Tsai, C.-H.; Wong, K.-T.; Huang, T.-W.; Hsieh, L.; Liu, S.-H.; Lin, H.-W.; Wu, C.-C.; Chou, S.-H.; Chen, S.-H.; Tsai, A.-I. *J. Org. Chem.* **2010**, *75*, 4778 and references cited therein.
3. (a) Jung, H.; Hwang, H.; Park, K.-M.; Kim, J.; Kim, D.-H.; Kang, Y. *Organometallics* **2010**, *29*, 2715. (b) Park, H.; Rao, Y.; Varlan, M.; Kim, J.; Ko, S.-B.; Wang, S.; Kang, Y. *Tetrahedron* **2012**, *68*, 9278.
4. (a) Yamaguchi, S. *Synth. Met.* **1996**, *82*, 149. (b) Zeng, W.; Cao, Y.; Bai, Y.; Wang, Y.; Shi, Y.; Zhang, M.; Wang, F.; Pan, C.; Wang, P. *Chem. Mater.* **2010**, *22*, 1915.
5. (a) Wang, Z.-S.; Hara, K.; Dan-oh, Y.; Kasada, C.; Shinpo, A.; Suga, S.; Arakawa, H.; Sugihara, H. *J. Phys. Chem. B* **2005**, *109*, 3907. (b) Wang, X.-F.; Kitao, O.; Zhou, H.; Tamiaki, H.; Sasaki, S.-I. *J. Phys. Chem. C* **2009**, *113*, 7954.
6. Milne, J. E.; Buchwald, S. L. *J. Am. Chem. Soc.* **2004**, *126*, 13028.
7. Ko, S.; Choi, H.; Kang, M.-S.; Hwang, H.; Ji, H.; Kim, J.; Ko, J.; Kang, Y. *J. Mater. Chem.* **2010**, *20*, 2391.
8. Lee, J.-H.; Liu, Q.-D.; Bai, D.-R.; Kang, Y.; Tao, Y.; Wang, S. *Organometallics* **2004**, *23*, 6205.
9. Details are deposited in ESI.
10. Nazeeruddin, M. K.; Zakeeruddin, S. M.; Humphry-Baker, R.; Jirousek, M.; Liska, P.; Vlachopoulos, N.; Shklover, V.; Fischer, C.-H.; Grätzel, M. *Inorg. Chem.* **1999**, *38*, 6298 .